Journal of
Marine Science and Engineering

MDPI

Article

A Vector Sensor-Based Acoustic Characterization System for Marine Renewable Energy

Kaustubha Raghukumar *, Grace Chang, Frank Spada and Craig Jones

Integral Consulting Inc, Santa Cruz, CA 95062, USA; gchang@integral-corp.com (G.C.); fspada@integral-corp.com (F.S.); cjones@integral-corp.com (C.J.)

* Correspondence: kraghukumar@integral-corp.com; Tel.: +1-831 466 9630

Received: 9 January 2020; Accepted: 6 March 2020; Published: 10 March 2020

Abstract: NoiseSpotter is a passive acoustic monitoring system that characterizes, classifies, and geo-locates anthropogenic and natural sounds in near real time. It was developed with the primary goal of supporting the evaluation of potential acoustic effects of offshore renewable energy projects. The system consists of a compact array of three acoustic vector sensors, which measures acoustic pressure and the three-dimensional particle velocity vector associated with the propagation of an acoustic wave, thereby inherently providing bearing information to an underwater source of sound. By utilizing an array of three vector sensors, the application of beamforming techniques can provide sound source localization, allowing for characterization of the acoustic signature of specific underwater acoustic sources. Here, performance characteristics of the system are presented, using data from controlled acoustic transmissions in a quiet environment and ambient noise measurements in an energetic tidal channel in the presence of non-acoustic flow noise. Data quality is demonstrated by the ability to reduce non-acoustic flow noise contamination, while system utility is shown by the ability to characterize and localize sources of sound in the underwater environment.

Keywords: marine renewable energy; acoustics; environmental characterization

1. Introduction

The market acceleration and adoption of marine renewable energy (MRE) technologies requires that hurdles related to their perceived environmental effects are better understood, characterized, and mitigated [1,2]. A key environmental stressor of concern is the acoustic impacts of MRE, given that sound is an important mechanism via which marine animals find prey, communicate, and engage in social behavior. With ongoing progress in MRE device development, there is a growing concern over noise levels emanating from these devices. Sound emissions related to MRE devices are regulated by the National Oceanic and Atmospheric Administration National Marine Fisheries Service [3], which sets limits on appropriately weighted sound pressure levels above which sound emissions can be considered detrimental to marine mammals. As a consequence, and because determining actual noise levels in the marine environment is difficult and often cost-prohibitive, a number of notable efforts to measure and monitor noise from MRE devices are under development.

Haxel et al. [4] recently tested a real-time acoustic observing system (RAOS) that consists of a surface telemetry buoy coupled to a bottom-mounted, self-powered acoustic hydrophone and modem package. The bottom-mounted hydrophone unit archives and relays processed acoustic data digests via an acoustic communication link to a surface buoy, from where it is transmitted, via a satellite link to a land-based station. With the bottom device and surface buoy, RAOS requires a doubling of deployment and recovery effort, with the further constraint that the measurement consists of only a single spatial measurement of acoustic pressure. To obtain location estimates of MRE devices, the developers proposed the simultaneous deployment of four RAOS devices around a wave

energy converter installation. This approach, similar to Greene et al. [5], offers considerable acoustic travel-time differences for location estimates of low-frequency sound. Location estimates, however, are not available in real time, and the presence of independent processing units can lead to difficulties with clock synchronization.

Rush et al. [6] developed a tethered underwater remotely operated vehicle (ROV) with a suite of oceanographic sensors including a hydrophone, a sonar system, cameras, velocimeter, and current profiler. This futuristic integrated monitoring system includes a bottom-mounted cabled docking station. While the ROV is designed to make mobile acoustic measurements in the immediate vicinity of an MRE device, the presence of a tether can cause unwanted complications when operating in the vicinity of MRE devices consisting of several berths, connected with tendon-like cables. Additionally, given the low noise emitted by MRE devices, the presence of multiple thrusters and ballast pumps can significantly reduce the signal-to-noise ratio, a problem common in glider-based acoustic measurement platforms [7]. Furthermore, location estimation using a single pressure-only hydrophone remains a challenge, and the engineering costs involved in designing, maintaining, and deploying an ROV can be significant.

Polagye et al. [8] developed a low-cost drifting acoustic instrumentation system that can be deployed as small swarms around MRE devices to measure and localize device sound. By virtue of being drifting units, contamination by flow noise is significantly reduced in high-current regions, while a heave plate provides vertical stabilization in wave-dominated environments. However, the drifting nature makes long-term operational measurements cumbersome, if not impossible, while the use of hydrophones requires the use of several drifting units for accurate source localization.

Two vector-sensor based acoustic monitoring systems that were employed to provide location estimates of vocalizing baleen whales are those designed by Greene et al. [5] and D'Spain et al. [9]. These systems, with vector sensors spaced several kilometers apart [5] or that contain a single vector sensor [9] are not fit-for-purpose systems built to monitor and measure MRE noise. They lack real-time onboard processing and data transmission capabilities, and they do not take advantage of advances in low-cost vector sensor technology.

NoiseSpotter is a newly developed monitoring technology to support the evaluation of potential environmental effects of MRE devices. The technology seeks to improve upon traditional acoustic sensing techniques through integration of a compact array of acoustic vector sensors with custom data dissemination technologies to characterize, classify, and provide accurate location information, in near real time, for anthropogenic and natural sounds. Traditional acoustic sensing techniques typically involve the use of hydrophones that measure scalar acoustic pressure. Consequently, acoustic source localization typically requires the use of large arrays consisting of multiple hydrophones [10]. The large size and footprint of hydrophone arrays can, therefore, make it difficult to deploy using a small vessel in energetic environments near operational MRE devices. An attractive alternative to the use of large hydrophone arrays is the use of compact arrays of acoustic vector sensors. A vector sensor measures three-dimensional (3D) acoustic particle velocity in addition to acoustic pressure on a single sensor, which inherently provides directional information (acoustic bearing) to a source of sound. A vector sensor array (VSA) can, therefore, triangulate individual measured bearings to provide sound source localization, thereby helping to characterize sounds specific to a source. MRE devices are expected to emit low-intensity operational sounds on the order of 110–130 decibels (dB) referenced to 1 microPascal (re 1 µPa) at 1 m [11]. These levels are considerably lower than sounds from other anthropogenic activities such as shipping or pile-driving that are known to exceed 180 dB re 1 µPa. Therefore, in order to characterize MRE sounds, it is important to be able to distinguish it from other sources of sound such as boats, marine mammals, and fish choruses. Furthermore, given the increasing interest on acoustic particle velocity effects on fishes and invertebrates [12], the particle motion measurements afforded by a VSA can play an important role in further understanding this aspect of acoustic propagation.

The objectives of this paper are to (1) describe technological aspects of the 'a newly developed system called the NoiseSpotter including results from in-water field measurements and (2) demonstrate

the utility and feasibility of vector sensors to locate a known, controlled acoustic source. These objectives help address key knowledge gaps regarding noise levels of MRE devices. These knowledge gaps, once addressed, can help potentially mitigate concerns about the acoustic effects of MRE on marine animals, paving the way for a more sustainable and equitable utilization of MRE resources.

2. Materials and Methods

The system hardware, electronics, and field trials are described in the sub-sections below.

2.1. Hardware

The NoiseSpotter's VSA hardware system consists of a 1.25 m × 1.25 m fiberglass grate with three high-density polyethylene (HDPE) modular frames, each housing a vector sensor draped in custom flow noise shields (Figure 1). An optional mooring line connects the bottom platform to a surface buoy for recovery, while an optional Ethernet cable connects the data logger to the surface buoy to facilitate real-time telemetry of data digests via cellular, radio frequency, or satellite communication. A third option for the VSA hardware system is replacement of the mooring line and surface buoy with an acoustic release and pop-up buoy system for system recovery.

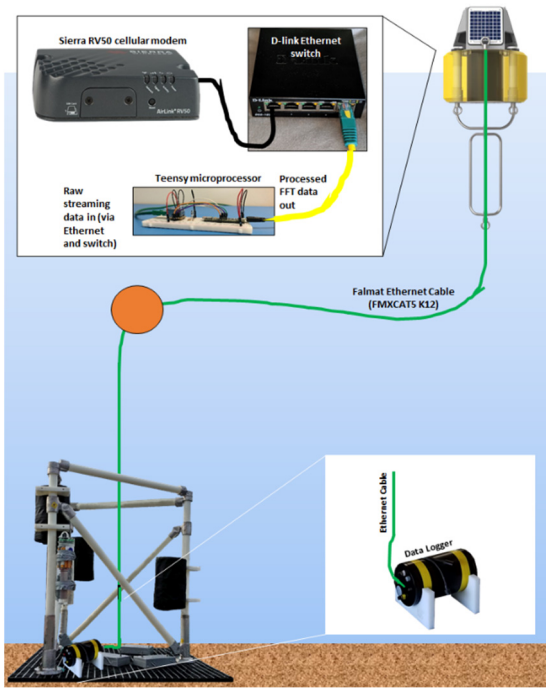

Figure 1. Schematic of NoiseSpotter.

The VSA's individual frames to house each vector sensor enable adjustment of horizontal and vertical spacing between the three vector sensors. The horizontal spacing of the system can be a maximum of 80 cm, while the vertical spacing can be a maximum of 40 cm, noting that these limitations may be exceeded with customized hardware solutions. The modularity of the system allows the system configuration to be tuned to particular frequencies of interest while minimizing spatial aliasing that can occur when the half-wavelength is smaller than the array spacing. For example, location estimates of lower-frequency sounds (<1 kHz) require at least 1-m horizontal spacing for sensors, whereas a more compact and hand-deployable arrangement of sensors can be used to geolocate higher-frequency sounds. The use of HDPE allows for improved acoustic transparency, while minimizing the potential for low-frequency acoustic scattering by other more commonly used materials such as stainless steel or aluminum that have an acoustic impedance significantly different from that of seawater. The acoustic

impedance of seawater is nominally 1.572 g/cm^2·s, while the acoustic impedances for aluminum, steel, and HDPE are 17.10, 45, and 2.937 g/cm^2·s, respectively [13].

The flow noise shields, developed in collaboration with Noise-Control Engineering, are constructed of 1050 ballistic nylon wrapped around a baffled poly-vinyl chloride (PVC) tube inside which a vector sensor is suspended. Extensive laboratory tests of 1050 ballistic nylon revealed that it is acoustically transparent and significantly reduces flow inside the noise shield. Therefore, reduction in flow noise is expected due to reduction of flow inside the shield. Furthermore, because of its acoustic transparency, VSA-measured acoustic signals are not affected. Biofouling field tests indicated that the flow noise shields largely resisted marine growth for a period of approximately three weeks in shallow, productive marine waters. Anti-fouling paints applied to 1050 ballistic nylon mitigated the effects of biofouling for up to six weeks.

The electronics system consists of three vector sensors and a data logger. The three vector sensors are from Geospectrum Technologies Ltd. (Dartmouth, Nova Scotia, Canada): two model M20-40s and one M20-100. The vector sensors are rated to a 200 m water depth. The M20-40 features a single wet-connect underwater cable that relays the four analog measurement fields (tri-axial particle velocity and omni-directional pressure) to an external amplifier circuit board. The M20-100 operates similarly to the M20-40, but is augmented with a second wet-connect underwater cable and digital amplifier circuit board to receive the digital compass output from the sensor. Power to the vector sensors is supplied via an amplifier circuit board connected to a rechargeable battery pack (32 Ahr; Sartek Industries Inc.), and it is relayed to the sensors via the wet-connect underwater cable.

The acoustic vector sensors are sensitive to acoustic frequencies in the 50 Hz–3 kHz range, with a flat frequency response on the pressure channel, and a peak in the response at 1 kHz on the particle velocity channels. This frequency range is particularly suited to measurement of sounds from MRE installations that primarily emit sound below 500 Hz [11] and marine mammals whose hearing sensitivities fall within this frequency range (50 Hz–3 kHz). Examples of marine mammals that primarily vocalize in (and are, therefore, sensitive to) this frequency range are the larger cetaceans that include mysticete whales and sperm whales (specific species include the blue whale, fin whale, gray whale, Bryde's whale, right whales, minke whales, bowhead whales, humpback whales, sei whales, and beaked whales) [14]. The nominal pressure sensitivity of the pressure channel at 1 kHz is −179 dB re V/μPa, which, along with the saturation level of the sensors, allows for measurement of sound pressure levels up to 240 dB re 1 μPa at a distance of 100 m from the sensor. This level is well above sound pressure levels that can cause permanent threshold shifts in marine mammal hearing [3].

A custom low-noise, low-power data logger was designed to synchronously sample multiple analog and digital compass channels. Twelve analog channels (x, y, z, and pressure for three sensors) of time-synchronized VSA data at 24 bits and one digital channel (orientation) are recorded by the custom data logger at a synchronous sampling rate of 20 kHz per channel. Analog sensor output is converted to a digital format, and all data are stored on a solid-state drive. The data logger, in a stainless steel pressure housing, is mounted on the bottom fiberglass grate.

The NoiseSpotter is designed to operate autonomously for up to three weeks without servicing. In-water tests indicate that the hardware configuration is suitable for small-vessel (8 m) operations in quiescent, energetic, and deep-water environments.

2.2. Field Testing

A series of field trials were conducted in and near Sequim Bay, Washington in July 2018 in collaboration with the Pacific Northwest National Laboratory (PNNL). The field sites (Figure 2) represented a quiescent shallow site (SB2, water depth 26 m) and an energetic tidal channel (Marine Sciences Laboratory (MSL), water depth 7–10 m). NoiseSpotter system performance was tested with the goals of evaluating data quality, ease of deployment and recovery, flow noise removal, and performance of the location estimation algorithm. At each location, the NoiseSpotter was deployed on the sea bottom, with an inverse catenary mooring to the sea surface such that surface-induced motions are

decoupled from the sensor platform. A controlled acoustic source (icTalk®, Ocean Sonics Ltd.) was deployed over the side of the vessel, the R/V Strait Science, at 1 m below the sea surface, and it was programmed to repeatedly transmit a series of low-frequency pulsed sinusoids, followed by chirps. The acoustic signals spanned the frequency range 100 Hz to 3 kHz, at a source level of 120 dB re 1 µPa at 1 m. Testing at the SB2 location typically involved the repeated transmission of the controlled acoustic signals at source–receiver separations of 50 m, 200 m, 500 m, and 1000 m. Due to the more involved effort required to moor the vessel in the energetic tidal channel at MSL, the vessel was allowed to drift past the sensor platform to/from a distance of 500 m, while continuously transmitting the controlled acoustic signals. Additionally, ambient noise measurements were made at all locations to characterize the noise floor, to evaluate flow noise contributions, and to assist in acoustic propagation modeling.

Figure 2. Map of NoiseSpotter testing locations.

3. Results

Results from the various field trials are presented from the point of view of data quality (low electronic/self-noise), adequate signal-to-noise ratio, and flow noise removal efficiency.

3.1. Data Quality

Pressure and particle velocity data are presented for the controlled acoustic source transmissions at SB2, a source of opportunity (a passing boat) at the SB2 location, and ambient noise spectra at MSL to demonstrate data quality.

3.2. Signal to Noise Ratio

Figure 3 shows the low-frequency pulsed and swept acoustic transmissions, as received on the NoiseSpotter's VSA when deployed at SB2, at a distance of 200 m from the controlled source. Transmitted signals are clearly discernible, and any artefacts due to electronic and self-noise such as spectral lines are not evident. Low-frequency ambient noise below 1000 Hz is also evident and generally free of self-noise artefacts. Horizontal spectral lines indicative of electronic noise exhibit a far lower signal-to-noise ratio than signals from the controlled source; vertical motions induced by cable strum are also absent from data (Figure 3). The quality of data recorded by the custom data logger is observed to be very high and suitable for location estimation without further data filtering.

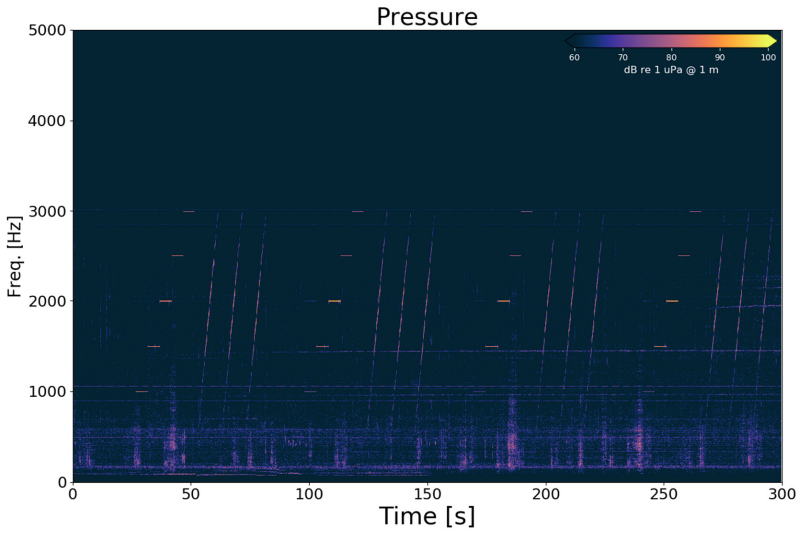

Figure 3. Pressure as measured on a single vector sensor in 26-m-deep water at the SB2 location, Sequim Bay, Washington, United States of America (USA).

Figure 4 shows particle velocity measurements made on the x-channel of one of the NoiseSpotter's vector sensors, the M20-40. The unique acoustic signature of a passing boat is seen as the characteristic parabolic Lloyd's mirror interference pattern for passing vessels [15], generated as the interference between the surface-reflected and direct path to a bottom receiver, where the width of the parabola and size of interference bands are dependent on the waveguide geometry and water column properties. In addition to the interference pattern, spectral lines characteristic of a boat's propeller blade cavitation are also visible, lending further confidence in the technology's low self-noise, allowing for measurement of ambient sounds.

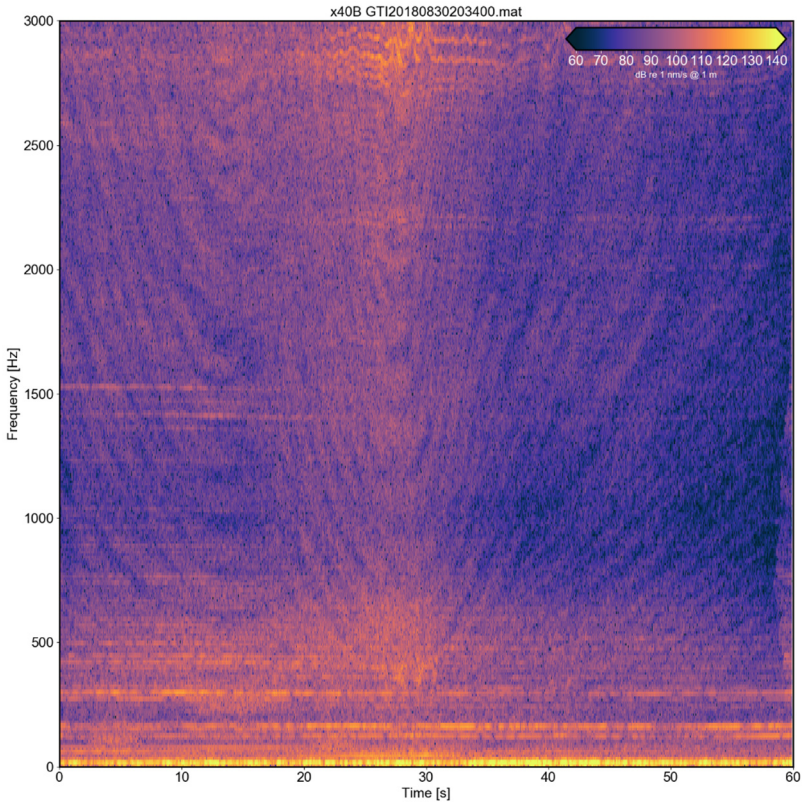

Figure 4. Particle velocity on x-channel of vector sensor M20-40, measured at the SB2 location.

3.3. Flow Noise Removal

The NoiseSpotter was deployed at the mouth of Sequim Bay in Washington, United States of America (USA) (MSL in Figure 2) on a bottom platform in a water depth of 8 m with respect to the mean sea level. This location is an energetic tidal channel, where the tidal excursion during the deployment was 2.5 m. Ambient noise was recorded on the VSA between approximately 6:30 a.m. and 8:00 p.m. Pacific Standard Time (PST), covering one complete tidal cycle. In this paper, sensor data from the M20-100 are analyzed for flow noise contamination, which is typically indicated by increased spectral levels below 500 Hz [16]. The flow shield was in place during a dropping tide (Figure 5), and it was removed from the PVC baffle during the subsequent rising tide. Therefore, any improvements in flow noise suppression would be indicated by lower spectral intensity levels below 500 Hz when a flow shield is deployed around the sensor.

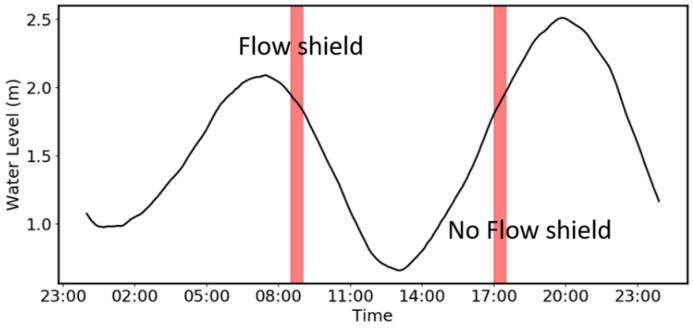

Figure 5. Tidal water level over the course of the field test on 30 August 2018. Highlighted regions indicate NoiseSpotter deployments with, and without the flow noise removal shield.

Particle velocity and pressure ambient noise frequency spectra were calculated with and without the flow noise removal shield. Improvements in flow noise reduction are seen in the primary flow noise frequency band of 0–500 Hz on the pressure, x-, and z-particle velocity channels (Figure 6). In this frequency band, flow noise reductions are seen to be on the order of 10–15 dB. Little to no change is observed for the y-particle velocity channel, attributed to the flow being orthogonal to the y-axis.

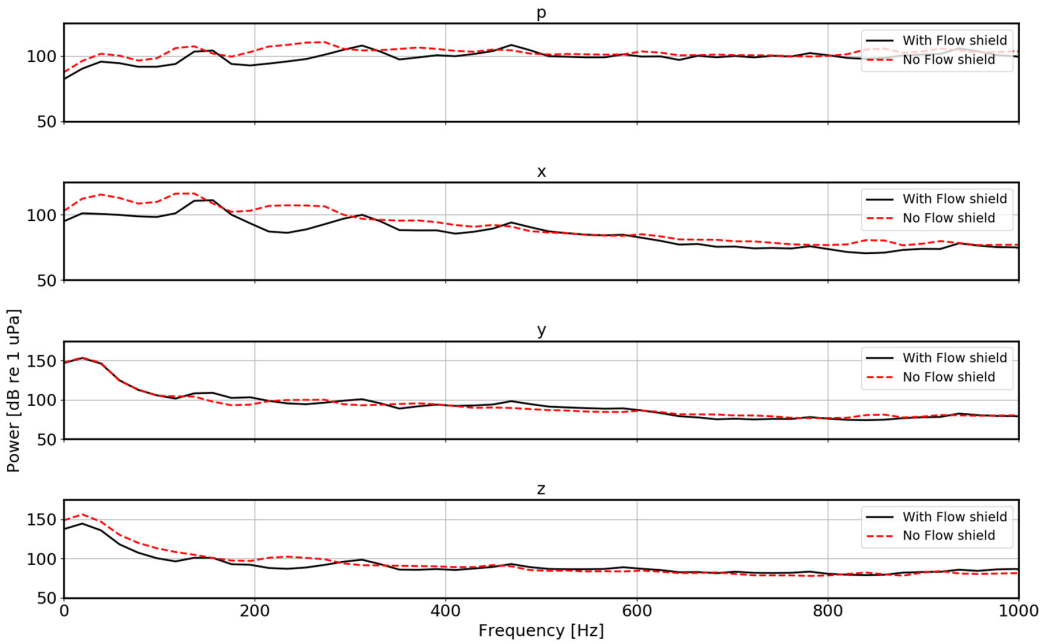

Figure 6. Ambient noise frequency spectra for the pressure and particle velocity channels, with and without the flow shield.

A number of metrics to describe non-acoustic contributions to acoustic propagation, such as flow noise, can be derived using VSA data. Vector sensor measurements consist of four measured quantities that represent acoustic pressure and particle velocity, represented as A(x,t) = [p, vx, vy, vz], where the particle velocity components are expressed in units of pressure via the scaling ρc, where ρ is the density of seawater (1000 kg/m^3), and c is the nominal speed of sound in seawater (1500 m/s). The density of seawater and speed of sound in water are environmental variables that determine sound propagation in the ocean. The choice of constant values is a simplification that can contribute to the error variance of any processed metrics, including location estimates. Velocity components are typically measured in a local frame of reference and transformed to an earth-based frame of reference using Eulerean angles measured by an in-built or collocated inertial motion unit. The Fourier transform of the time series in $\mathbf{A}(x,t)$ is given by $\mathbf{A}(x,\omega)$. The cross-spectral density matrix $\mathbf{S}(\omega)$ is then given by the ensemble-averaged outer product of the vector $\mathbf{A}(x,\omega)$. Individual components of the cross-spectral density matrix can be expressed as $\mathbf{S}_{ij}(x,\omega) = \mathbf{A}_i(x,\omega)\ \mathbf{A}_j^*(x,\omega)$. Assuming ergodicity, $\mathbf{S}(x,\omega)$ can be calculated by averaging successive snapshots of $\mathbf{A}(x,\omega)$ computed over an interval of time. $\mathbf{S}(x,\omega)$ can then be decomposed into its real and imaginary components as $\mathbf{S}(x,\omega) = \mathbf{C}(x,\omega) + i\,\mathbf{Q}(x,\omega)$, where $\mathbf{C}(x,\omega)$ and $\mathbf{Q}(x,\omega)$ represent the in-phase and quadrature components of the individual elements of the cross-spectral density matrix. For example, the off-diagonal elements $\mathbf{S}_{1j}(x,\omega)$ represent the pressure-velocity cross-spectra whose in-phase and quadrature elements are related to physical quantities that represent acoustic power flow [17]. The in-phase components $\mathbf{C}_{1j}(x,\omega)$, termed the active intensity, represent the net power being propagated by the acoustic field. The quadrature component, $\mathbf{Q}_{1j}(x,\omega)$, termed the reactive intensity, relates pressure and particle velocity components that are orthogonal to each other, and it represents spatially heterogeneous power flow [17].

Non-acoustic contamination may be evaluated through the reactive intensity components of the cross-power spectral density matrix. For example, a metric to evaluate the contribution of the non-acoustic component on the x-particle velocity channel can be defined [18] that arises from the relationship between the particle velocity cross-spectra and active and reactive intensity vectors.

$$M_{21} = \frac{\left|Q_{34}(\omega)\right| - \left|\left(\frac{C_{1[2,3,4]}(\omega)\times Q_{1[2,3,4]}(\omega)}{S_{11}(\omega)}\right)_x\right|}{\left|Q_{34}(\omega)\right| + \left|\left(\frac{C_{1[2,3,4]}(\omega)\times Q_{1[2,3,4]}(\omega)}{S_{11}(\omega)}\right)_x\right|}. \quad (1)$$

The notation $\mathbf{X}_{1[2,3,4]}$ represents the off-diagonal elements of the matrix $\mathbf{X}$, arranged as a vector, and × is the vector cross-product. Values of M_{2j} that deviate significantly from zero are considered to be a flag of non-acoustic contamination. Similar to M_{21}, metrics for the other particle velocity channels (M_{22}, M_{23}) can be defined.

The probability distribution of M_{21} (Equation 1) was computed for NoiseSpotter VSA data collected at MSL over a 30-min period during each tidal cycle, as shown in Figure 7. A marked contrast is seen in the distributions with and without the flow shields. Distributions with the flow shield (right half of Figure 7) are seen to cluster around zero between 0 and 250 Hz, and no significant deviations toward higher values are observed. In contrast, the M_{2j} distributions without the flow shield (left half of Figure 7) are seen to cluster toward a value of 1 over much of the 0–500 Hz range shown, indicating the presence of non-acoustic signal contamination.

3.4. Location Estimation

A key principle of long-distance underwater acoustic propagation is that sound travels along discrete paths between a source and a receiver. Given the uniqueness of the acoustic field between a source and receiver, a variety of techniques can be employed to determine the location of a sound source [10]. These techniques vary in hardware complexity, accuracy, and computational efficiency based on the underlying physical assumptions. The NoiseSpotter is a platform that can improve upon the method of direction of arrival estimation by using acoustic vector sensors that measure triaxial

particle velocity in addition to acoustic pressure. Each vector sensor has the ability to determine the bearing of an acoustic source. With multiple time-synchronized vector sensors located on the array, the essential principle of the proposed technology is that the source can be geo-located by triangulation of particle velocity vectors measured across the array [5,19].

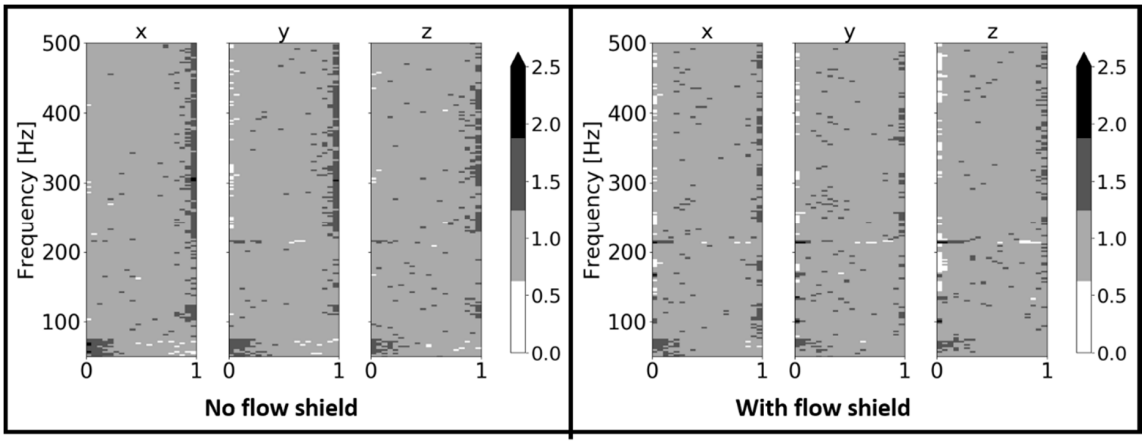

Figure 7. Probability distribution of M2j metric, with and without a flow shield.

The basic principle of triangulation using the NoiseSpotter's vector sensor array is illustrated in Figure 8. Here, a plane wave impinges upon a linear array of acoustic sensors. For a given angle of incidence, the signal received on each channel of the acoustic array is offset by a frequency-dependent phase relative to that received on neighboring channels. Plane-wave beamforming [20] acts by phase-shifting the signal on each channel, followed by coherently summing over the array. A larger number of array channels result in a greater array gain, as well as better suppression of incoherent random noise, while reinforcing a coherent signal. A vector sensor makes four acoustic measurements on each sensor. Therefore, a vector sensor array can exhibit four times the array gain of a traditional hydrophone array with the same number of physical sensors.

Having established adequate data quality of the acoustic monitoring system, bearing estimation of the acoustic source was demonstrated. The technique for bearing estimation calculation involves segmenting time series of NoiseSpotter VSA data into discrete 1-s-long segments (20,000 points at a sampling frequency of 20 kHz). Then, 1024-point fast Fourier transforms (FFTs) are computed on each 1-s data segment, and plane-wave beamforming is applied in the frequency domain following the methods outlined by Santos et al. [20]. At each frequency bin, this method yields a dominant azimuth and elevation angle for each time segment, estimates of which are then stitched together for the entire time series.

Bearing estimation was conducted for multiple 6-min-long time series of controlled acoustic source transmissions that were obtained at various source receiver separations (10 m, 50 m, 100 m, 500 m, and 1 km) during in-water field testing. Figure 9 shows an example of elevation and angle estimates obtained for a 3-min-long time series, when the source was located 180 m from the receiver. Shown in the upper panel is a spectrogram of the received signal, which shows the evolution of the frequency content of received signals. Receptions of the controlled source transmissions are seen as the step-like progression in energy across frequency as an evolution of time. The frequency-domain beamforming processing is performed for the tone at 1700 Hz, selected to demonstrate that specific tones can be geolocated, while ignoring sources at other frequencies. Estimates of azimuth and elevation angle during these periods are seen to closely track the true bearing of the source. Outside of these periods where the source was transmitting, the bearing angles exhibit significantly larger deviations from the true bearing, consistent with isotropic ambient noise that has no dominant direction. Having estimated the three-dimensional bearing angle to the source, the true location of the source (Figure 10) is estimated assuming a known source depth. This assumption is valid when trying to associate

measured signals with MRE devices, whose locations are usually known in the water column. The estimated source location is seen to be co-located with the true source location, with an estimation error of 3.6 m or 2% of the source–receiver separation distance.

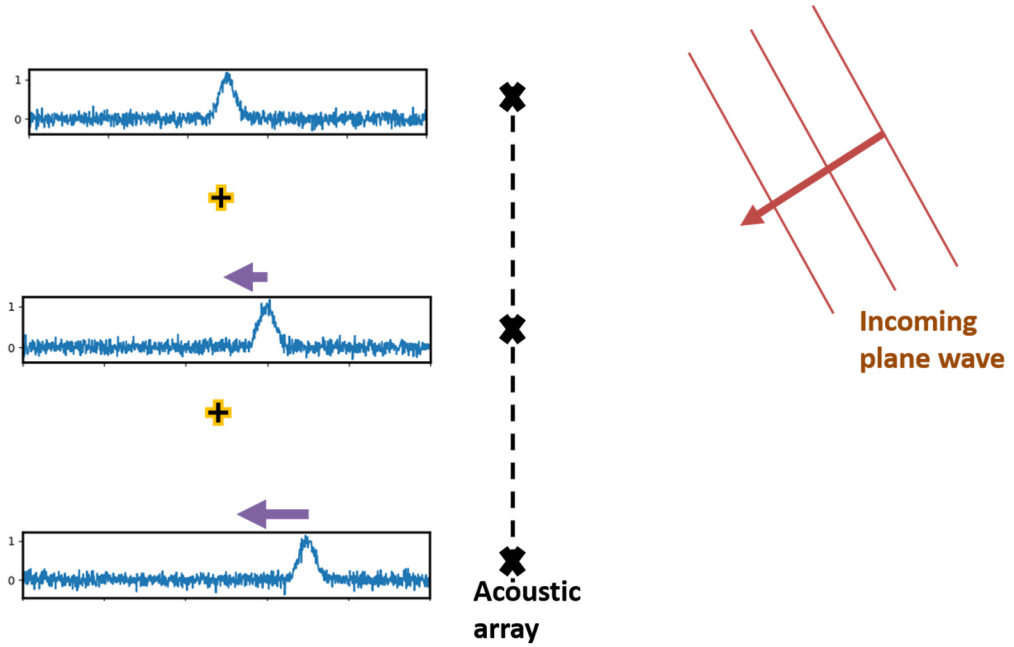

Figure 8. Principle of plane-wave beamforming applied to an acoustic array.

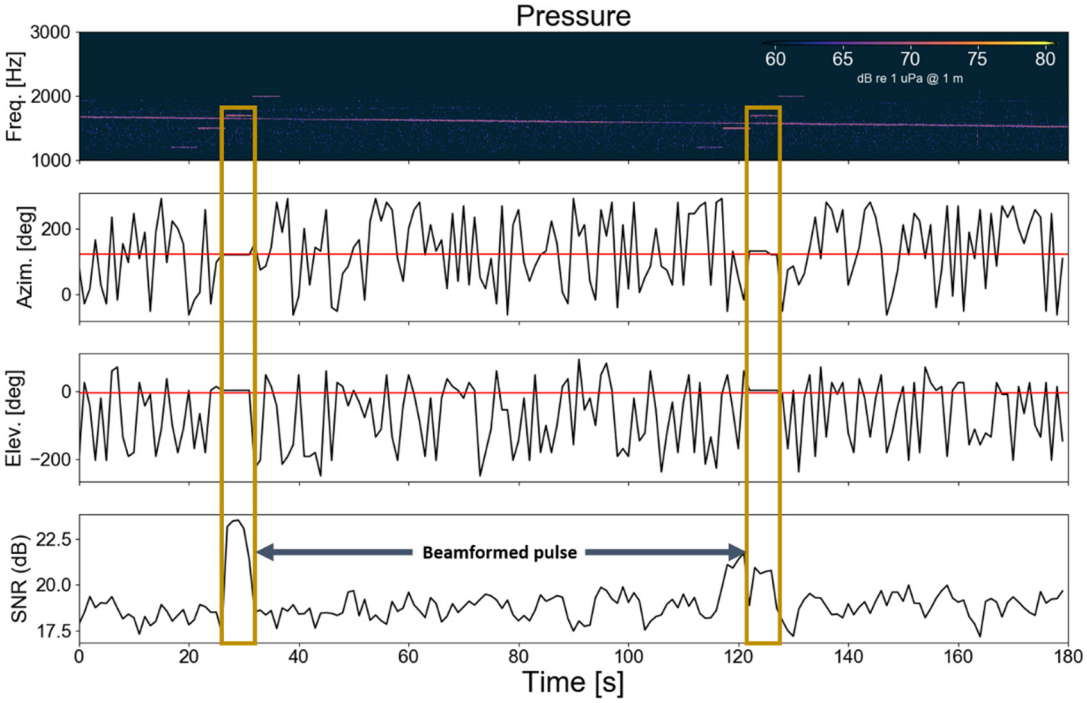

Figure 9. Beamforming location estimation algorithm applied to a 5-min data segment collected in August 2018. Source pulses of interest at 1700 Hz are outlined in orange.

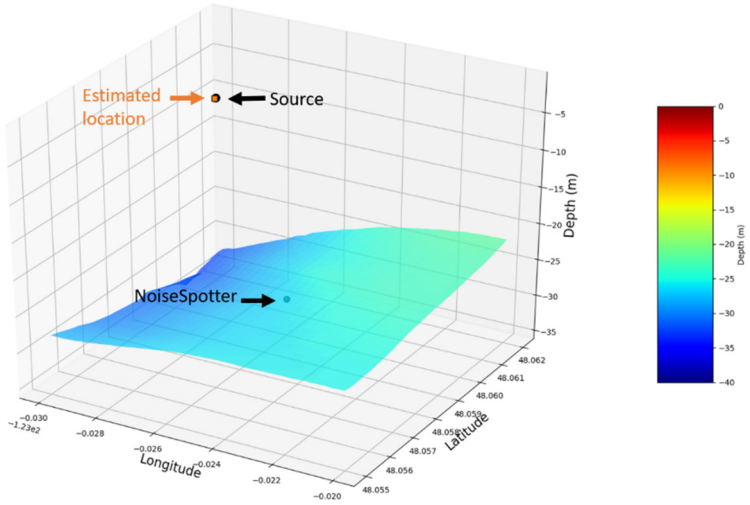

Figure 10. True (black) and estimated (orange) controlled source locations relative to the NoiseSpotter V3 (blue), which were separated from the source by 200 m. The difference between true and estimated locations is 3.6 m (2% of separation distance).

4. Discussion and Summary

Ocean ambient noise levels appear to be increasing worldwide, as a result of increasing anthropogenic activities (e.g., shipping, seismic surveys, and pile-driving) [21], ocean acidification [22], and global economic growth, thereby further decreasing the ability of marine animals to communicate, find prey, and socialize [23]. In recognition of its identified importance, underwater sound is now a key ocean variable, along with the more well-known quantities such as temperature, salinity, and density [24]. Several large international efforts are now underway to identify and quantify long-term trends in underwater noise levels, such as the Oslo Paris (OSPAR) convention [25], Marine Strategy Framework Initiative, and the Joint Monitoring Program for Ambient Noise North Sea (JOMOPANS) [26]. In light of these efforts, the acoustic monitoring technology described in this paper can better help identification of noise sources through its localization capability, and it can pave the way for improved characterization of acoustic particle velocity, which is the acoustic quantity of interest to fishes and marine invertebrates [27].

Acoustic vector sensors are in use since the 1950s [28], primarily as the acoustical sensing unit on board US Navy directional sonobuoys for anti-submarine warfare. The utility of these sensors to localize acoustic sources such as baleen whales and ships was explored by a few studies [5,10,20,29]. More recently, the importance of particle motion in coral reef soundscapes and its significance to fish were explored [30,31], and these findings contributed to the increasing awareness of its biological significance. However, widespread commercial application was hampered to date by the affordability of reasonably priced sensors, lack of documentation, and challenges in suppressing motion-induced noise (flow noise) and electronic self-noise, as well as the limited application of an array of vector sensors. This paper, therefore, presents an advancement of the state of the science by developing and applying a three-dimensional array of vector sensors to monitor a variety of underwater sounds. The key scientific advancements are as follows:

- Development of a three-dimensional vector sensor array using a modular frame whose acoustic impedance is very close to that of seawater;
- Quantitative characterization of flow noise contamination, and its suppression in an energetic channel, applied to a vector sensor;
- Application of a location estimation algorithm to an in-water acoustic source.

The development of a modular hardware system based on a fiberglass bottom platform upon which an HDPE frame is mounted allows for a unit whose acoustic impedance is much closer to that of

seawater than other commonly used materials such as aluminum or stainless steel, thereby minimizing the possibility of acoustic scattering by the frame itself. While improper mounting of acoustic vector sensors can often result in unwanted motion of the sensor (see Reference [32] and references therein), the use of PVC pods with a robust, repeatable mounting system provides high data quality as evidenced by the measurements of nearby vessel traffic with little to no data contamination. The use of a three-dimensional array allows for inter-element separation of sensors in both the horizontal and vertical direction. This has the potential to reduce spatial aliasing through the use of multiple array spacings [10]. A horizontal array spacing of 75 cm allows for aliasing-free beamforming at frequencies of 1000 Hz or lower, while the vertical spacing of 25 cm allows for aliasing-free beamforming at frequencies of 3000 Hz or lower.

The contamination of acoustic measurements by non-acoustic pressure fluctuations can be induced either from ambient flow or from the relative motion between the sensor and surrounding fluid [9]. An acoustic flow suppression shield acts as a physical barrier between the turbulence-inducing flow and the hydrophone, while remaining acoustically transparent. Flow noise contamination can be particularly confounding when using vector sensors, since these sensors measure acoustic particle motion using accelerometers that physically respond to the propagation of an acoustic wave. In this paper, a flow shield made of ballistic nylon was found to be an effective suppressor of flow noise for a vector sensor in an energetic tidal flow, with flow noise suppression on the order of 10–15 dB. However, it is noted that, while the flow shield does result in flow noise suppression (Figures 6 and 7), the suppression is not total. This is evident in some deviation toward higher values in the M_{2j} metric, even in the presence of a flow shield, indicating residual non-acoustic contamination. In highly energetic current environments, where flow noise can exceed 50 dB [16], work remains to be done in further suppressing flow noise contamination.

Finally, plane-wave beamforming techniques were applied to the vector sensor data to obtain the three-dimensional bearing to a source at a known depth, which was then used to infer its location. The application of beamforming to locate a source using an array of hydrophones along with complex acoustic propagation models is a rich field with a long history [33]. The utility of the bearing information, inherent to vector sensor measurements, allows for three-dimensional low-frequency source localization which previously required large two-dimensional hydrophone arrays. Beamforming of vector sensor array data to locate a ship was recently demonstrated [20], and it was applied here to locate a sub-surface source, albeit at a known depth. It was found that, while errors in source location were less than 4 m with a 200-m source–receiver separation (2% error), achieving this error requires careful measurement of location of the vector sensor spacing. Furthermore, it is critical that the inertial motion unit is properly calibrated to allow for the accurate translation of relative azimuth and bearing estimates into true earth coordinates.

The NoiseSpotter described in this paper ties together all the above work to provide a new tool for commercial noise assessments, useful for the MRE industry, as well as for any application that requires geolocation of acoustic sources below 3 kHz. Typical sources of sound in this frequency range include wave and tidal energy converters, baleen and mysticete whales, ships, and low-frequency sonar.

5. Conclusions

This paper presented the performance characteristics of the NoiseSpotter, an easily deployable self-logging vector sensor array. The results of field trials were presented in a variety of environments that showed excellent data quality in each of these environments with regard to discerning controlled source transmissions and sources of opportunity. The ability to mitigate flow noise, key in energetic environments, was demonstrated in a tidal channel, with approximately 10–15-dB reduction of flow noise at 200 Hz. The in-water tests indicate that the hardware configuration is suitable for small-vessel (8 m) operations in quiescent, energetic, and deep-water environments.

The ability of the system to estimate the location of a source of sound was demonstrated using plane-wave beamforming techniques applied to a vector sensor array. The compact size of the vector

sensor array allows for beamforming array gain comparable to much larger hydrophone arrays, and location estimates of the controlled source were found to be within 2% of the source–receiver separation.

Next steps involve further improvements in the flow noise removal ability. Further progress on the location estimation algorithm will revolve around estimating the true location of a source without any assumptions regarding source depth, while taking into account multipath reflections that can be expected with longer-range acoustic propagation.

Author Contributions: Conceptualization, K.R., G.C., and C.J.; methodology, K.R.; software, K.R.; validation, K.R., G.C., and F.S.; formal analysis, K.R. and G.C.; investigation, K.R., G.C., and F.S.; resources, C.J.; data curation, G.C. and K.R.; writing—original draft preparation, K.R.; writing—review and editing, K.R. and G.C.; visualization, K.R.; supervision, C.J.; project administration, G.C.; funding acquisition, K.R., G.C., and C.J. All authors have read and agreed to the published version of the manuscript.

Funding: This material is based upon work supported by the US Department of Energy's Office of Energy Efficiency and Renewable Energy (EERE) under the Water Power Program Award Number DE-EE0007822.This presentation was prepared as an account of work sponsored by an agency of the United States Government. Neither the United States Government nor any agency thereof, nor any of their employees, makes any warranty, express or implied, or assumes any legal liability or responsibility for the accuracy, completeness, or usefulness of any information, apparatus, product, or process disclosed, or represents that its use would not infringe privately owned rights. Reference herein to any specific commercial product, process, or service by trade name, trademark, manufacturer, or otherwise does not necessarily constitute or imply its endorsement, recommendation, or favoring by the United States Government or any agency thereof. The views and opinions of authors expressed herein do not necessarily state or reflect those of the United States Government or any agency thereof.

Acknowledgments: The authors extend their gratitude to the Pacific Northwest National Laboratory Marine Science Laboratory (PNNL MSL) for field support. Sean Griffin (Proteus Technologies LLC) and Jesse Spence (Noise-Control Engineering) were invaluable for hardware design and testing. Brendan Nichols and Karim Sabra (Georgia Tech) and Jit Sarkar and Bill Hodgkiss (Scripps Institution of Oceanography) provided feedback on design. The authors would like to specially thank Brian Polagye and his laboratory (University of Washington) for valuable acoustic discussions and continued collaborations. The authors also thank Jesse Roberts, Kelley Ruehl, Sharon Kramer, and Pete Nelson for help in evaluating the utility of NoiseSpotter for MRE applications.

Conflicts of Interest: The authors declare no conflicts of interest. The funders had no role in the design of the study; in the collection, analyses, or interpretation of data; in the writing of the manuscript, or in the decision to publish the results.

References

1. Copping, A.; Sather, N.; Hanna, L.; Whiting, J.; Zydlewski, G.; Staines, G.; Gill, A.; Hutchison, I.; O'Hagan, A.; Simas, T.; et al. Annex IV 2016 State of the Science Report: Environmental Effects of Marine Renewable Energy Development Around the World. *Ocean Energy Syst.* **2016**, 224.
2. Roche, R.C.; Walker-Springett, K.; Robins, P.E.; Jones, J.; Veneruso, G.; Whitton, T.A.; Piano, M.; Ward, S.L.; Duce, C.E.; Waggitt, J.J.; et al. Research priorities for assessing potential impacts of emerging marine renewable energy technologies: Insights from developments in Wales (UK). *Renew. Energy* **2016**, *99*, 1327–1341. [CrossRef]
3. National Marine Fisheries Service. *2018 Revisions to: Technical Guidance for Assessing the Effects of Anthropogenic Sound on Marine Mammal Hearing (Version 2.0): Underwater Thresholds for Onset of Permanent and Temporary Threshold Shifts*; NOAA Technical Memorandum NMFS-OPR-59; US Department of Commerce, NOAA: Silver Spring, MD, USA, 2018; p. 167.
4. Haxel, J.; Turpin, A.; Matsumoto, H.; Klinck, H. A portable, real-time passive acoustic system and autonomous hydrophone array for noise monitoring of offshore wave energy projects. In Proceedings of the Marine Energy Technology Symposium, Washington, DC, USA, 25 April 2016.
5. Greene, C.R., Jr.; McLennan, M.W.; Norman, R.G.; McDonald, T.L.; Jakubczak, R.S.; Richardson, W.J. Directional frequency and recording (DIFAR) sensors in seafloor recorders to locate calling bowhead whales during their fall migration. *J. Acoust. Soc. Am.* **2004**, *116*, 799–813. [CrossRef] [PubMed]
6. Rush, B.; Stewart, A.; Joslin, J.; Polagye, B. Development of an adaptable monitoring package for marine renewable energy projects Part 1: Conceptual design and operation. In Proceedings of the 2nd Marine Energy Technology Symposium, Global Marine Renewable Energy Conference, Seattle, WA, USA, 18 April 2014.
7. Chandrayadula, T.; Miller, C.W.; Joseph, J. Monterey Bay ambient noise profiles using underwater gliders. *Proc. Meet. Acoust.* **2013**, *19*, 070031.

8. Polagye, B.; Noe, J.; Crisp, C.; Cotter, E.; Murphy, P. Drifting Acoustic Instrumentation for Marine Energy, Poster. In Proceedings of the International Conference on the Environmental Interactions of Marine Energy Technologies, Orkney, UK, 24–27 April 2018.
9. D'Spain, G.L.; Hodgkiss, W.S.; Edmonds, G.L. The simultaneous measurement of infrasonic acoustic particle velocity and acoustic pressure in the ocean by freely drifting Swallow floats. *IEEE J. Ocean. Eng.* **1991**, *16*, 195–207. [CrossRef]
10. Thode, A.; D'Spain, G.L.; Kuperman, W.A. Matched-field processing, geoacoustic inversion, and source signature recovery of blue whale vocalizations. *J. Acoust. Soc. Am.* **2000**, *107*, 1286–1300. [CrossRef] [PubMed]
11. Tougaard, J. Underwater noise from a wave energy converter is unlikely to affect marine mammals. *PLoS ONE* **2015**, *10*. [CrossRef]
12. Hawkins, A.D.; Popper, A.N. Assessing the impact of underwater sound on fishes and other forms of marine life. *Acoust. Today* **2014**, *10*, 30–41.
13. NDT Resource Center. Available online: https://www.nde-ed.org/GeneralResources/MaterialProperties/UT/ut_matlprop_index.htm (accessed on 14 February 2020).
14. Mellinger, D.K.; Stafford, K.M.; Moore, S.E.; Dziak, R.P.; Matsumoto, H. An overview of fixed passive acoustic observation methods for cetaceans. *Oceanography* **2007**, *20*, 36–45. [CrossRef]
15. McKenna, M.; Wiggins, S.M.; Hildebrand, J.A. Underwater radiated noise from modern commercial ships. *J. Acoust. Soc. Am.* **2012**, *92*, 92–103. [CrossRef]
16. Bassett, C.; Thomson, J.; Dahl, P. Flow noise and turbulence in two tidal channels. *J. Acoust. Soc. Am.* **2014**, *135*, 1764–1774. [CrossRef] [PubMed]
17. D'Spain, G.L. Energetics of the Deep Ocean's Infrasonic Sound Field. Ph.D. Thesis, University of California, San Diego, CA, USA, 1990.
18. Thode, A.; Skinner, J.; Scott, P.; Roswell, J. Tracking sperm whales with a towed acoustic sensor. *J. Acoust. Soc. Am.* **2010**, *128*, 2681–2694. [CrossRef] [PubMed]
19. Nehorai, A.; Paldi, E. Acoustic vector sensor array processing. *J. Acoust. Soc. Am.* **1994**, *51*, 1479–1491. [CrossRef]
20. Santos, P.; Felisberto, P.; Hursky, P. Source localization with vector sensor array during the Makai experiment. In Proceedings of the 2nd International Conference and Exhibition on "Underwater Acoustic Measurements: Technologies and Results", Heraklion, Greece, 25–29 June 2007; pp. 895–900.
21. Merchant, N.; Brookes, K.; Faulkner, R.; Bicknell, A.W.J.; Godley, B.J.; Witt, M.J. Underwater noise levels in UK waters. *Sci. Rep.* **2016**, *6*, 36942. [CrossRef]
22. Hester, K.C.; Peltzer, E.T.; Kirkwood, W.J.; Brewer, P.G. Unanticipated consequences of ocean acidification: A noisier ocean at lower pH. *Geophys. Res. Lett.* **2008**, *35*, L19601. [CrossRef]
23. National Research Council. *Ocean Noise and Marine Mammals*; The National Academies Press: Washington, DC, USA, 2003.
24. The Global Ocean Observing System. Available online: https://www.goosocean.org/index.php?option=com_content&view=article&id=14&Itemid=114 (accessed on 14 February 2020).
25. OSPAR Commission. Available online: https://www.ospar.org/ (accessed on 14 February 2020).
26. Joint Monitoring Program for Ambient Noise North Sea. Available online: https://northsearegion.eu/jomopans/ (accessed on 14 February 2020).
27. Nedelec, S.L.; Campbell, J.; Radford, A.N.; Simpson, S.D.; Merchant, N.D. Particle motion: The missing link in underwater acoustic ecology. *Methods Ecol. Evol.* **2016**, *7*, 836–842. [CrossRef]
28. Holler, R.A. *The Evolution of the Sonobuoy from World War II to the Cold War*; No. JUA-2014-025-N; NAVMAR APPLIED SCIENCES CORP: Warminster, PA, USA, 2014.
29. McDonald, M.A. DIFAR hydrophone usage in whale research. *Can. Acoust.* **2004**, *32*, 155–160.
30. Kaplan, M.; Mooney, T. Coral reef soundscapes may not be detectable far from the reef. *Sci. Rep.* **2016**, *6*, 31862. [CrossRef]
31. Horodysky, A.Z.; Brill, R.W.; Fine, M.L.; Musick, J.A.; Latour, R.L. Acoustic pressure and particle motion thresholds in six sciaenid fishes. *J. Exp. Biol.* **2008**, *211*, 1504–1511. [CrossRef]

32. McConnell, J.A. Analysis of a compliantly suspended acoustic velocity sensor. *J. Acoust. Soc. Am.* **2003**, *113*, 1395. [CrossRef] [PubMed]
33. Brienzo, R.K.; Hodgkiss, W.S. Broadband matched-field processing. *J. Acoust. Soc. Am.* **1993**, *94*, 2821–2831. [CrossRef]